ACTA METALLURGICA SLOVACA
2021, VOL. 27, NO. 2, 47-52

RESEARCH PAPER

MICROSTRUCTURE, MECHANICAL AND TRIBOLOGICAL BEHAVIOUR OF AISI 316L STAINLESS STEEL DURING SALT BATH NITRIDING

Elhadj Ghelloudj [1*]

[1] *Department of industrial mechanics, SH/DP Regional Direction Haoud Berkaoui, Ouargla 30000, Algeria*

*Corresponding author: hadjhadj105@gmail.com, tel.: +213676407456, *Department of industrial mechanics, SH/DP Regional Direction Haoud Berkaoui, Ouargla 30000, Algeria*

Received: 26.04.2021
Accepted: 08.05.2021

ABSTRACT

The current work aimed to analyze the impact of salt bath nitriding on the behavior of the tribological characteristics and surface microstructures of AISI 316L stainless steels. Nitriding was carried out at 580 °C for 10 h. The tribological, structural behavior of the AISI 316L before and after salt bath nitriding was compared. The surface microstructures, tribological characteristics, as well as its surface hardness, were investigated using optical microscopy (OM), X-ray diffractometer (XRD), surface profilometer, pin-on-disk wear tester, and microhardness tester. In the current work, the experimental results showed that a great surface hardness could be achievable through the salt bath nitriding technique because of the formation of the so-called expanded Austenite (S-phase), the nitrogen diffusion region. The surface hardness of AISI 316 stainless steel after the nitriding process reached 1100 HV0.025 which was six times the untreated sample hardness. The S-phase is additionally expected to the improvement of wear resistance and decrease the friction coefficient.

Keywords: AISI 316L stainless steel; Friction coefficient; Salt bath nitriding; Surface hardness; S-phase; Wear resistance

INTRODUCTION

Austenitic stainless steel is one of the four categories of stainless steel alloy: austenitic [1], ferritic [2], martensitic and duplex [3, 4]. The austenitic group of stainless steel has a major composition of chromium, nickel, manganese steel, and minor amounts of other additional alloy elements [5, 6]. Because of their exceptionally high toughness [7], good ductility [8,9], formability [10], thermal conductivity [11], good welding properties [12], nonmagnetic properties [13], high impact energy, and great corrosion resistance [14-16] they are widely used in applications of low-temperature technology [17] such as orthopedic [18] industries, ocean technology [19], aerospace [20], food processing equipment [21], nuclear reactors [22, 23], manufacturing of several parts of automotive [24], petrochemical processing [25], etc.

Austenitic stainless steels, which incorporate the AISI 316L stainless steel, have many applications in the industry due to their good mechanical characteristics and their exceptional corrosion resistance [26], especially in certain environments. Low hardness and poor wear resistance [27] are some of the main drawbacks of austenitic stainless steels and are therefore subject to various types of surface characteristics failure [28]. Because of the limited tribological properties of these alloys (poor wear resistance), their scope of industrial applications was limited [29]. Several studies have shown that nitriding treatment has produced a hard surface layer resulting in improved wear resistance. Thus, the nitriding treatment is a perfect alternative for raising the surface hardness, This ensures the efficacy of the wear resistance characteristic when this is required in service [30]. Nitriding is one of the forms of surface treatments used to improve the surface properties of materials [31]. This technique also improves the hardness, mechanical properties, and fatigue strength, and wear and corrosion resistance of various tools [32]. According to [33], nitriding is a thermochemical process through which nitrogen atoms are diffused and dispersed at the surface level of the materials at a proper temperature, which leads to an increase in the surface hardness and as a result increases the performance and the life span of the industrial parts. There are different methods of nitriding operations such as salt bath nitriding (SBN) [34-36], gas nitriding (GN) [37, 38], and plasma nitriding (PN) [39, 40]. A literature survey can easily find several hundred papers published over the last few years on the topic of nitriding of austenitic stainless steel [41-43]. The most common nitriding techniques are a salt bath with a nitrogen concentration-rich medium. This thermochemical process has been used to creating the required properties on the surface of stainless steels as such wear [44], fatigue [45], corrosion [46], and friction properties [47]. The medium used in salt bath nitriding is a salt that contains nitrogen, such as cyanide salt, or potassium nitrate. Salt baths with cyanide have the same, or even greater, nitrogen potential than ammonia. The nitriding behavior can be defined fairly through the diffusion of nitrogen into the parts. Most nitrogen is interstitially absorbed during nitriding. Minor oxidation was observed following nitriding. It can be considered a nitrocarburizing treatment since the salts used often typically contribute carbon to the surface of the workpiece, and the two elements generally permeate into the surface of the industrial parts [48]. There have been researched studies of the effects of nitriding treatments on the behavior of surface microstructure and characteristics of austenitic stainless steel such as AISI 304 [49,50], AISI 304L [51], AISI 321 [52], AISI 201 [53], AISI 316 [54], AISI 316L [55,56], AISI 202

[57], AISI 316LN [58] and AISI 316LVM [59], AISI 310[60], AISI 303[61], AISI 204[62]. However, there is a lack of research about the surface microstructural and tribological behavior of AISI 316L stainless steel during salt bath nitriding by the Tenifer process (TF1) at 580 °C. Therefore, in the present work, the structural and tribological behavior of AISI 316L stainless steel before and after salt bath nitriding (Tenifer) was investigated. The tribological properties and surface structures formed during nitriding were investigated using X-ray diffraction (XRD), microhardness tester, pin-on-disk wear test, surface profilometer, and optical microscopy (OM). The primary objective of the present study is to investigate the effect of salt bath nitriding by the Tenifer process (TF1) at 580 °C on tribological properties and surface microstructure of AISI 316L stainless steel.

MATERIALS AND METHODS

Material and salt bath nitriding processes

The material used in the present research was AISI 316L austenitic stainless steel with the chemical composition shown in Table 1. The specimens for the experiment were machined into dimensions of 30 mm × 10 mm × 5 mm.

Table 1 The chemical compositions of the AISI 316L used in this study (wt %)

C	Si	Mn	P	S	Mo	Cr	Ni	Fe
0.02	0.52	1.52	0.029	0.024	2.09	16.76	10.14	bal

The salt bath nitriding by Tenifer treatments was performed in a DEGUSSA furnace. A small gap was made in each sample with a diameter of about 2 mm, which could be attached to the end of a metal wire for easier get her out of the furnace. As usual, when processing required parts in the industry by salt bath nitriding (Tenifer TF1), The AISI 316L stainless steel samples were preheated to 350 °C for 30 min in preheating tank oven, after that nitriding process was performed at 580 °C for 10 h in the salt bath comprising of cyanates (36 ± 2 %), carbonates (19 ± 2 %) and cyanides (0.8 %). There is a reaction between the molten salt and the AISI 316L stainless steel specimens being processed during the salt bath nitriding process so that nitrogen and carbon are absorbed and diffused through the surfaces of the specimen.

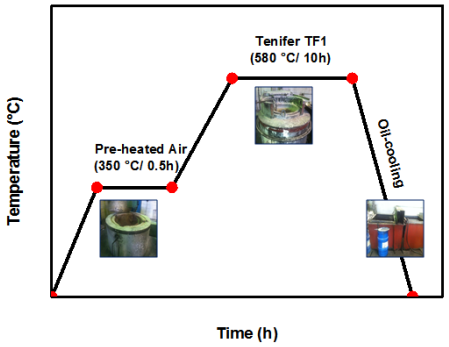

Fig. 1 Temperature - time plot for salt bath nitriding treatment

The emerging nitrogen used for the reaction of nitriding treatment coming out of the dissociation of Cyanate: $4CNO^- \rightarrow CO_3^{-2} + 2CN^- + CO + 2[N]$. The gradual change in the concentration between the surface of the specimen and the nitriding salt bath turns out to be the main thrust for the effective nitrogen atom to penetrate an austenite structure, which leads to the formation of a surface nitride layer. At the same time, a few emerging carbons, which come out during the dissociation of Carbon monoxide: $2CO \rightarrow CO_2 + [C]$, also penetrates austenite structure along with nitrogen. The parameters and processing of nitriding treatment are illustrated in Fig. 1.

Characterizations of the surface treatments

The samples treated with salt bath nitriding were analyzed using optical microscopy examination, microhardness measurements, X-ray diffraction analysis, surface profilometer, and wear tests under dry conditions. The microstructure on the cross-section of nitrided samples was analyzed after metallographic preparation and etching with 2% NITAL (2% HNO_3 in ethanol). The surface microstructure analysis was investigated by optical microscopy (GA-120). Measurements of microhardness profiles were obtained before nitriding using a microhardness tester fitted with a Vickers indentation with a load of 25 gf. This was also used for surface hardness measurements of the specimens treated. Averaging at least 3 measurements was used to determine the hardness value of samples. The surface profilometer was used for measuring and analyzing the surface roughness of treated and untreated specimens of AISI 316L stainless steel. According to ISO 4287:1997 standard, surface roughness was defined by measuring the parameters of surface roughness (Ra, Rq, and Rz). The tribological behaviors (friction and wear) of untreated and treated specimens of 316L stainless steel were evaluated under unlubricated condition by a pin-on-disk tribometer, in which the sample (disc) was rotated against a stationary steel ball as the pin of 5 mm diameter with a speed of 60 revs/min at a load of 5 N. The weight loss of the sample was evaluated using an electronic balance accurate to 0.1 mg.

RESULTS AND DISCUSSION

Surface microstructure analyses

Fig. 2 displays the cross-section microstructure of the sample of AISI 316L stainless steel, which was treated at the salt bath nitriding temperature of 580 °C for 10 h. As shown in the figure, the Tenifer nitrided surface (Researchers call it the "expanded austenite" or " S-phase) appears to have a multi-phase structure judged from the variations in layer composition. The average thickness of this layer was about 72 µm. A clear boundary existed between the top layer and the inner layer, the upper layer made up of a hardened layer of around 6 µm depth, accompanied by a slightly etched layer of around 66 µm depth. Further, the topmost layer (Rich in nitrogen) was bright, while the inner layer was completely darkened due to the Nital etching. Possibly the dark zone in the inner layer is caused by precipitation from CrN. This result ties well with previous studies wherein Gui et al. [63] detailed the nitrided morphology of AISI 316LSS using the optical microscope at 580 °C for 2h under salt bath nitrocarburizing. It was shown that the surface layer consists of Cr2N/ γ'-Fe_4N and CrN/ γ -Fe. In another study, Jiang et al. [64] detailed the surface microstructure of AISI 316 produced during salt bath nitrocarburizing but at low temperature (480 °C) for 6 h. They observed that the S-phase was formed and this nitrocarburized matrix zone was darkened after Nital etching.

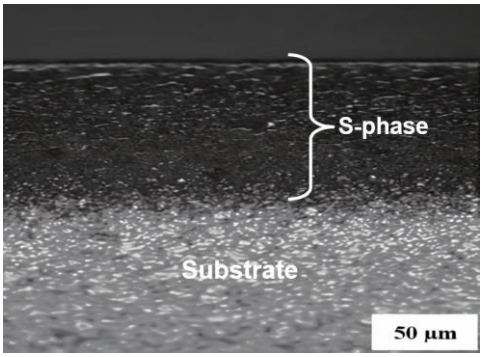

Fig. 2 Typical optical micrographs of the cross-section of AISI 316L after nitriding at 580 °C for 10h

Fig. 3 below illustrates a comparison of the XRD diffraction pattern of AISI 316 stainless steel between the sample that was treated by salt bath nitriding and the untreated sample. It has been shown to the untreated sample has a Face Centred Cubic crystal structure (γ-Fe) which was expected because the Austenitic stainless steels possess austenite as their primary crystalline structure (face-centered cubic). The nitrided sample at 580 °C has been characterized by the appearance of other phases, where a set of peaks, which do not match any existing ASTM X-ray diffraction index was distinguished. These peaks in this figure correspond to the S-phase (γN), chromium nitride phase (CrN), and formation of Fe_4N compound.

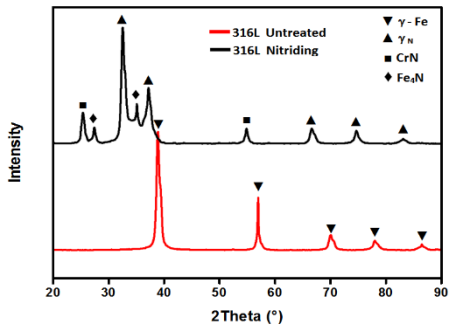

Fig. 3 Typical X-ray diffraction patterns of AISI 316 L SS before and after salt bath nitriding at 580 °C for 10h

It can be seen that the corresponding peaks of the expanded austenite phase are broadened and turned to lessen angles compared to peaks of untreated austenitic stainless steel. The crystal structure of the S-phase also has a face-centered cubic structure, the S-phase was formed due to the incorporation of the nitrogen atoms in the interstitial positions and gaps of the austenite structure. Overall these findings are following results reported by many studies [55, 56].

In addition, the appearance of CrN nitride at 580 °C. It was consistent with the conclusions stated in [53], which noted that at relatively high temperatures CrN nitride is favorably precipitated. The formation of CrN could be explained in the following form: Chromium appears as a solid solution in austenite steel, which emerges as the temperature increases of solid solution due to the contrast between the thermal properties of iron and chromium [65]. Furthermore, the comparatively low concentration of CNO^- (approximately 36%) in the cyanide-cyanate during the Tenifer (TF1) process is likely that the cause for the formation of the γ'-Fe_4N compound rather than the ε-Fe_2 (N, C).

Surface hardness profile

Fig. 4 shows the microhardness profiles presented as a function of the depth of AISI 316L stainless steel after the salt bath nitriding process by the Tenifer method (at 580 °C for 10h). As can see, the maximum microhardness obtained is up to 1100 HV0.025, while the substrate possesses a microhardness of approximately 200 HV0.025. Besides that, according to the graph, it can be seen that the hardness decreases progressively as the depth increases until it approaches hardness values to those of the untreated sample. The increase in hardness as a result of the gas nitriding process has been reported previously by Mahmoud et al. [66], where they found that the AISI 316L after the nitriding process have greater microhardness than compared to the untreated sample. A value surface hardness of about 1400 HV0.025 of the AISI 316L during nitrocarburizing has also been reported by Pinedo et al. [67].

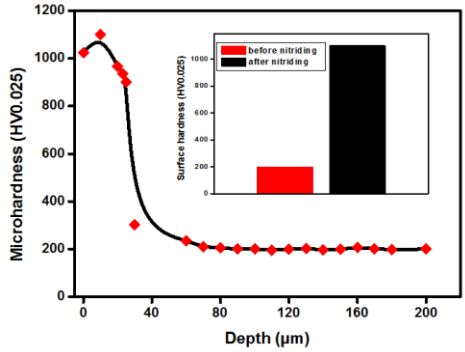

Fig. 4 Hardness profiles in the surface layer of the specimen after salt bath nitriding for 10h at 580 °C

Diffuse nitrogen has strong properties to improve material hardness. Both the hardness values and the nitrogen concentration decreased monotonously with increasing depth of the treated sample surface [68]. The high content of nitrogen is dissolved in austenite (S-phase), in which intensive precipitation of chromium nitride subsists, which significantly improves the hardness property. According to Fader et al. [69], the increase in nitride layer hardness is attributable to the higher nitrogen concentration, larger grain structure, and the appearance of expanded austenite in those regions. The core hardness values of the specimen nitrided before treated by salt bath nitriding were 200 HV0.025. It is noteworthy that the core hardness of the nitrided specimen was measured at the same level as for the specimen nitrided before nitriding in the salt bath (200 HV0.025). This confirms that during nitriding treatment the core of AISI 316Ldoes not soften by nitriding parameters (treatment time and temperature), i.e. microstructure of the core remains unchanged after nitriding of the salt bath.

Surface roughness measurement

Fig. 5 summarizes the average values of surface roughness parameters characterizing the surface topography (Ra, Rq, and Rz) of the untreated and treated samples, it can be observed an

important increase in the surface roughness values of the 316L stainless steel sample during the salt bath nitriding.

The average roughness value of arithmetic mean deviation of the roughness profile (Ra) of the sample nitrided was 0.366 µm, were higher almost 6 times than the average roughness of the sample before treatment. On the other hand, for the square mean deviation of the roughness profile (Rq), the roughness value was 0.574 µm, which was about 6.5 times higher than that of the untreated one. In addition to this, the roughness value of the maximum distance between the lowest and the highest points of the roughness profile (Rz) of the sample nitrided was 5.32 µm, which was about 3 times larger than the of the untreated sample. The increased surface roughness during salt bath nitriding can be attributed to the formation of the sliding bands on the nitrided sample due to the formation of the expanded austenite (S-phase). This result ties well with the previous study reported by Gajendra et al. [70] explained that the increased surface roughness of austenitic stainless steel during plasma nitriding could be due to the high chemical propagation average of hydrogen atoms by plasma in the nitrided layers especially the expanded austenite.

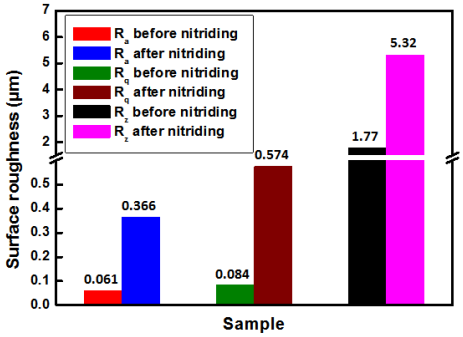

Fig. 5 Surface roughness parameters (Ra, Rq and Rz) before and after salt bath nitriding at 580 °C for 10h

Tribological characteristics

In this work, the friction behavior on the non-nitrided sample surface has been compared with those on the treated sample surface. The variation of friction coefficient measured against a steel ball is illustrated in Fig. 6 for the specimens of AISI 316L before and after salt bath nitriding in terms of rolling distance. At the beginning of the experiment, the coefficient of friction in both salt bath nitrided and untreated samples had a relatively high value, where the values of friction coefficients were 0.45 µm and 0.47 µm, respectively. This is due to the presence of initial static friction. After that, it was found in each sample that the coefficient of friction increased when the test time increases to a relatively constant value (by neglecting minor changes). The average friction coefficient values for the salt bath nitrided sample are approximately 0.486 µm while its value is approximately 0.528 µm for the untreated one.

From the results obtained, it can be said that the friction coefficient of the AISI 316L stainless steel sample was reduced utilizing surface hardening during salt bath nitriding as much as possible. In addition, the behavior of untreated material friction coefficient can be ascribed to adhesion wear that occurred as the result of increased contact temperature and welding points on the surface.

According to Zhang et al. [71], the low friction coefficient measured for the nitrided specimen can be credited to the increase of the surface hardness. Also, Yetim et al. [72] indicated that there in an S-phase with perfect friction-resistant properties in the surface microstructure of AISI 316L stainless steel after nitriding treatment which significantly reduces the values of the coefficient of friction.

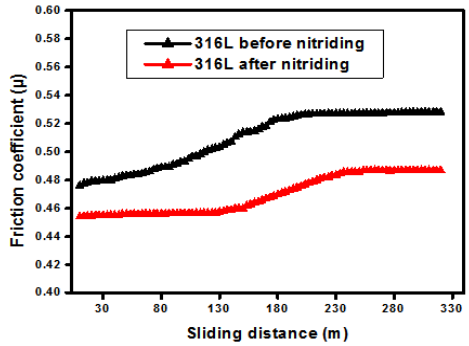

Fig. 6 Variations of friction coefficient of untreated and nitrided specimens of AISI 316L

Fig. 7 illustrates the results of the wear behavior of the nitriding treatment specimen of the AISI 316L compared with the untreated sample under the various dry sliding conditions were measured using a tribometer. It can be observed that, as predicted, the nitrided specimen had the highest wear resistance compared to the untreated one. for example, before salt bath nitriding the loss in weight increased 30 mg for 300 m of the sliding distance, while after salt bath nitriding the loss in weight increased 20 mg for 300 m of the sliding distance. This result ties well with previous studies wherein were confirmed that the resistance of wear resistance was attributable to the surface hardness of materials. Higher-hardness materials usually displayed greater wear resistance. According to Fig. 4, we know that the hardness of alloying elements nitride phase's fine particles (S-phase, CrN and γ' -Fe_4N) in the surface of nitrided sample during salt bath nitriding is more than 1100 HV0.025, that is about six times harder than that of the untreated one. Thus, the nitrided sample was expected to have better resistance to wear [73-76].

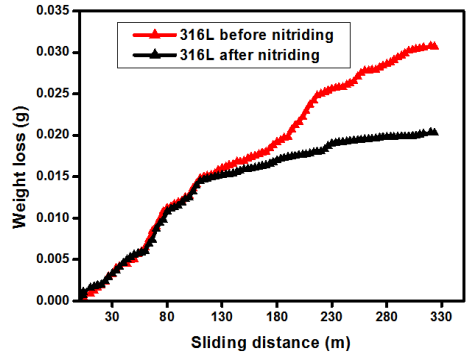

Fig. 7 Variation of weight loss against the sliding distance of AISI 316L SS before and after nitriding at 580 °C for 10h

CONCLUSION

The main goal of this work is to study the surface microstructure, tribological and mechanical behavior of AISI 316L austenite stainless steel at 580 °C during salt bath treatment by Tenifer processing (TF1). The results of this study can be summarized as:

The salt bath nitrided layer was composed of three sublayers, namely the CrN layer, the γ'-Fe_4N layer, and γ_N layer (S-phase).

The salt bath nitriding can very efficiently increase the hardness of the surface of AISI 316L. Maximum values obtained of the nitrided surface approximately 1100 HV0.025 for 10 h, which is around 6 times as hard as the untreated sample (200 HV0.025).

The surface roughness (Ra, Rq and Rz) is increased when compared with the "base material" condition after the salt bath nitriding by Tenifer processing.

The Tenifer process (TF1) can progress the resistance of wear and reduces the friction coefficient of the material under study.

ACKNOWLEDGMENTS

This research was supported by Sonatrach Haoud Berkaoui, Ouargla, Algeria and department of mechanical engineering, University Abbes Laghrour, Khenchela, Algeria

REFERENCES

1. S.H.Muhammad, N.S. Safaa, H. Esah, F.M. Moh.: Annales de Chimie - Science des Matériaux, 43(6), 2019, 369-375. https://doi.org/10.18280/acsm.430602
2. L.C. Gontijo, R.Machado, L.C. Casteletti, S.E. Kuri, P.A.P. Nascente: Materials Science Forum, 638-642, 2010, 775-780. https://doi.org/10.4028/www.scientific.net/msf.638-642.775
3. G. Prakash, S.K. Nath: Journal of Materials Engineering and Performance, 27(7), 2018, 3206-3216. https://doi.org/10.1007/s11665-018-3424-5
4. R. Huang, J. Wang, S. Zhong, M. Li, J. Xiong, H. Fan: Applied Surface Science, 271, 2013, 93-97. https://doi.org/10.1016/j.apsusc.2013.01.111
5. R.M. Oliveira, M. Ueda, I.H. Tan, L. Hoshida, C.B. Mello: Plasma Processes and Polymers, 4(S1), 2007, S655- S659. https://doi.org/10.1002/ppap.200731604
6. T. Czerwiec, H. He, G. Marcos, T. Thiriet, S. Weber, H. Michel: Plasma Processes and Polymers, 6(6-7), 2009, 401-409. https://doi.org/10.1002/ppap.200930003
7. K. Kwangyoon et al.: Metals, 8(11), 2018, 932 - 947. https://doi.org/10.3390/met8110932
8. J.C. Stinville, P. Villechaise, C. Templier, J.P. Riviere, M. Drouet: Surface and Coatings Technology, 204(12-13), 2010, 1947- 1951. https://doi.org/10.1016/j.surfcoat.2009.09.052
9. N. Karimzadeha, E.G. Moghaddam, M. Mirjani, K. Raeissi: Applied Surface Science, 283, 2013, 584-589. https://doi.org/10.1016/j.apsusc.2013.06.152
10. M.G. García et al.: Surface and Interface Analysis, 47(6), 2015, 728-737. https://doi.org/10.1002/sia.5770
11. W.M. Lima et al.: Journal of Physics: Condensed Matter, 17(7), 2005, 1239-1249. https://doi.org/10.1088/0953-8984/17/7/016
12. M. G. García et al.: Surface and Coatings Technology, 218, 2013, 142- 151. https://doi.org/10.1016/j.surfcoat.2012.12.043
13. A.S. Hamdy, B. Marx, D. Butt: Materials Chemistry and Physics, 126(3), 2011, 507-514. https://doi.org/10.1016/j.matchemphys.2011.01.037
14. I. Lee, A. Barua: Surface and Coatings Technology, 207, 2016, 1045-1052. https://doi.org/10.1016/j.surfcoat.2016.07.031
15. L.C. Gontijo, R. Machado, S.E. Kuri, L.C. Casteletti, P.A.P. Nascente: Thin Solid Films, 515(3), 2006, 1093-1096. https://doi.org/10.1016/j.tsf.2006.07.075
16. C.Y. Cui, J.D. Hu, Y.H. Liu, Z.X. Guo: Materials Science and Technology, 24(8), 2008, 964-968. https://doi.org/10.1179/174328408X322088
17. R. Bidulsky, et al.: Materials, 13(15), 2020, 3328. https://doi.org/10.3390/ma13153328
18. C.F. Hung, C.Z. Wu, W.F. Lee, K.L. Ou, C.M. Liu, P.W. Peng: Physics Procedia, 32, 2012, 914-919. https://doi.org/10.1016/j.phpro.2012.03.656
19. C. Paula et al.: Journal of Materials Research and Technology, 8(2), 2019, 1897-1906. https://doi.org/10.1016/j.jmrt.2019.01.006
20. M. Yakout, M.A. Elbestawi, S.C. Veldhuis: The International Journal of Advanced Manufacturing Technology, 95, 2018, 1953-1974. https://doi.org/10.1007/s00170-017-1303-0
21. D.S. Petrovič, D. Food and Bioproducts Processing, 100, 2016, 230-237. https://doi.org/10.1016/j.fbp.2016.07.006
22. T. Moskalioviene, A. Galdikas, J.P. Rivière, L. Pichon: Surface and Coatings Technology, 205(10), 2011, 3301- 3306. https://doi.org/10.1016/j.surfcoat.2010.11.060
23. P. Petrousek, et al: Acta Metallurgica Slovaca, 25(4), 2019, 283-290. https://doi.org/10.12776/ams.v25i4.1366
24. L. Ceschini, C. Chiavari, E. Lanzoni, C. Martini: Materials & Design, 38, 2012, 154-160. https://doi.org/10.1016/j.matdes.2012.02.019
25. Y.Y. Chen, Y.M. Liou, H.C. Shih: Materials Science and Engineering: A, 407(1-2), 2005, 114-126. https://doi.org/10.1016/j.msea.2005.07.011
26. K.H. Lo, C.H. Shek, J.K.L. Lai: Materials Science and Engineering R, 65(4-6), 2009, 39-104. https://doi.org/10.1016/j.mser.2009.03.001
27. M. Egawa, Y. Matsuda, N. Ueda, T. Sone, M. Tsujikawa, K. Nakata: Plasma Processes and Polymers, 6(S1), 2009, S893-S896. https://doi.org/10.1002/ppap.200932205
28. M. Peruzzo, F.L. Serafini, M.F.C. Ordoñez, R.M. Souza, M.C.M. Farias: Wear, 422-423, 2019, 108-118. https://doi.org/10.1016/j.wear.2019.01.027
29. C.E. Foerster et al.: Surface and Coatings Technology, 204(18-19), 2010, 3004-3008. https://doi.org/10.1016/j.surfcoat.2009.12.030
30. T. Watanabe, M. Kondo, A. Sagara: Electrochimica Acta, 58, 2011, 681-690. https://doi.org/10.1016/j.electacta.2011.10.014
31. S.K. Singh, C. Naveen, Y.V Sai, U. Satish, C. Bandhavi, R. Subbiah: Materials Today: Proceedings, 18, 2019, 2717-2722. https://doi.org/10.1016/j.matpr.2019.07.134
32. M. Dai, C. Li, J. Hu: Journal of Alloys and Compounds, 688, 2016, 350-356. https://doi.org/10.1016/j.jallcom.2016.07.189
33. Y.H. Qiang, S.R. Ge, Q.J. Xue: Journal of Materials Processing Technology, 101(1-3), 2000, 180-185. https://doi.org/10.1016/s0924-0136(00)00466-0
34. E. Ghelloudj, M.T. Hannachi, H. Djebaili: Acta Metallurgica Slovaca, 24(4), 2018, 280-286. https://doi.org/10.12776/ams.v24i4.1111
35. T. Peng, M. Dai, W. Cai, W. Wei, K. Wei, J. Hu: Applied Surface Science, 484, 2019, 610-615. https://doi.org/10.1016/j.apsusc.2019.04.134
36. W. Mei, J. Wu, M. Dai, K. Wei, J. Hu: Acta Metallurgica Slovaca, 25(2), 2019, 130-135. https://doi.org/10.12776/ams.v25i2.1271

37. A.R. Clauss, E. Bischoff, R.E. Schacherl, E.J. Mittemeijer: Materials Science and Technology, 26(3), 2010, 297-308. https://doi.org/10.1179/174328409x422266
38. P. Kochmański, J. Nowacki: Surface and Coatings Technology, 200(22-23), 2006, 6558-6562. https://doi.org/10.1016/j.surfcoat.2005.11.034
39. L. Wang, S. Ji, J. Sun: Surface and Coatings Technology, 200(16-17), 2006, 5067-5070. https://doi.org/10.1016/j.surfcoat.2005.05.036
40. E. Grigore, C. Ruset, X. Li, H. Dong: Plasma Processes and Polymers, 6(S1), 2009, S321-S325. https://doi.org/10.1002/ppap.200930703
41. L. Shen, L. Wang, J.J. Xu: Surface and Coatings Technology, 228, 2013, S456-S459. https://doi.org/10.1016/j.surfcoat.2012.05.026
42. S. Lu, X. Zhao, S. Wang, J. Li, W. Wei, J. Hu: Vacuum, 145, 2017, 334-339. https://doi.org/10.1016/j.vacuum.2017.09.020
43. E.D.L. Heras et al.: Plasma Processes and Polymers, 4(S1), 2007, S741-S745. https://doi.org/10.1002/ppap.200731809
44. D.C Wen: Wear, 268(3-4), 2010, 629-636. https://doi.org/10.1016/j.wear.2009.10.012
45. K. Funatani: Metal Science and Heat Treatment, 46(7-8), 2004, 277-281. https://doi.org/10.1023/b:msat.0000048834.48163.2e
46. K. Marušić, H. Otmačić, D. Landek, F. Cajner, E. Stupnišek-Lisac: Surface and Coatings Technology, 201(6), 2006, 3415-3421. https://doi.org/10.1016/j.surfcoat.2006.07.231
47. G. Pantazopoulos, P. Psyllaki, D. Kanakis, S. Antoniou, K. Papadimitriou, J. Sideris: Surface and Coatings Technology, 200(20-21), 2006, 5889-5895. https://doi.org/10.1016/j.surfcoat.2005.09.001
48. Y.Z. Shen, K.H. Oh, D.N. Lee: Scripta Materialia, 53(12), 2005, 1345-1349. https://doi.org/10.1016/j.scriptamat.2005.08.032
49. J. Wang, Y. Lin, Q. Zhang, D. Zeng, H. Fan: Metallurgical and Materials Transactions A, 45(10), 2014, 4525-4534. https://doi.org/10.1007/s11661-014-2418-7
50. X. Liu, C. Mao, M. Wu, W. Cai, M. Dai, J. Hu: Acta Metallurgica Slovaca, 26(1), 2020, 4-6. https://doi.org/10.36547/ams.26.1.458
51. G. Li et al.: Materials Characterization, 59(9), 2008, 1359-1363. https://doi.org/10.1016/j.matchar.2007.09.011
52. L. Bellas, G. Castro, L. Mera, J.L. Mier, A. García, A. Varela: Metal Science and Heat Treatment, 58(5-6), 2016, 369-375. https://doi.org/10.1007/s11041-016-0019-3
53. H.S. Luo, C. Zhao: Physics Procedia, 50, 2013, 38-42. https://doi.org/10.1016/j.phpro.2013.11.008
54. X. Zhang et al.: Metallurgical and Materials Transactions A, 49(1), 2018, 356-367. https://doi.org/10.1007/s11661-017-4382-5
55. M.F.C. Ordoñez et al.: Surface and Coatings Technology, 374, 2019, 700-712. https://doi.org/10.1016/j.surfcoat.2019.06.002
56. F. Borgioli: Metals, 10(2), 2020, 187-233. https://doi.org/10.3390/met10020187
57. F. Borgioli, E. Galvanetto, T. Bacci: Corrosion Science, 136, 2018, 352-365. https://doi.org/10.1016/j.corsci.2018.03.026
58. P. Rajendran, A. Devaraju: Materials Today: Proceedings, 5(6), 2018, 14333-14338. https://doi.org/10.1016/j.matpr.2018.03.016
59. E. Ura-Bińczyk, A. Krawczyńska, R. Sitek, M. Lewandowska: Surface and Coatings Technology, 375, 2019, 565-572. https://doi.org/10.1016/j.surfcoat.2019.07.035
60. R. Djellal, A. Saker, B. Bouzabata, D.E. Mekki: Surface and Coatings Technology, 325, 2017, 533- 538. https://doi.org/10.1016/j.surfcoat.2017.07.014
61. Y. Lin, W. Lan, K. Ou, C. Liu, P. Peng: Surface and Coatings Technology, 206(23), 2012, 4785- 4790. https://doi.org/10.1016/j.surfcoat.2012.03.089
62. D. Zeng, S. Yang, Z.D. Xiang: Applied Surface Science, 258(12), 2012, 5175-5178. https://doi.org/10.1016/j.apsusc.2012.01.167
63. G. Li et al.: Surface and Coatings Technology, 202(13), 2008, 2865-2870. https://doi.org/10.1016/j.surfcoat.2007.10.032
64. Z. Cheng, C.X. Li, H. Dong, T. Bell: Surface and Coatings Technology, 191(2-3), 2005, 195-200. https://doi.org/10.1016/j.surfcoat.2004.03.004
65. A. Fossati, F. Borgioli, E. Galvanetto, T. Bacci: Surface and Coatings Technology, 200(11), 2006, 3511-3517. https://doi.org/10.1016/j.surfcoat.2004.10.122
66. H.R.S. Mahmoud, S.A. Yusoff, A. Zainuddin, P. Hussain, M. Ismail, K. Abidin: MATEC Web of Conferences, 13, 2014, 4021-4025. https://doi.org/10.1051/matecconf/20141304021
67. C.E. Pinedo, A.P. Tschiptschin: International Heat Treatment and Surface Engineering, 5(2), 2011, 73-77. https://doi.org/10.1179/174951411x13051201040703
68. J.F. dos Santos, C.M. Garzón, A.P. Tschiptschin: Materials Science and Engineering: A, 382(1-2), 2004, 378-386. https://doi.org/10.1016/j.msea.2004.05.003
69. A. Feder, J. Alcalá, L. Llanes, M. Anglada: Journal of the European Ceramic Society, 23(15), 2003, 2955-2962. https://doi.org/10.4028/www.scientific.net/amm.529.251
70. P.S. Gajendra, J. Alphonsa, P.K. Barhai, P.A. Rayjada, P.M. Raole, S. Mukherjee: Surface and Coatings Technology, 200(20-21), 2006, 5807- 5811. https://doi.org/10.1016/j.surfcoat.2005.08.149
71. F. Zhang, M. Yan: Journal of Materials Science & Technology, 30(12), 2014, 1278-1283. https://doi.org/10.1016/j.jmst.2013.10.032
72. A.F. Yetim, M. Yazıcı: Journal of Bionic Engineering, 11(4), 2014, 620-629. https://doi.org/10.1016/s1672-6529(14)60073-1
73. B. Hashemi, M. Rezaee Yazdi, V. Azar: Materials & Design, 32(6), 2011, 3287-3292. https://doi.org/10.1016/j.matdes.2011.02.037
74. Y. Li, L. Wang, J.J. Xu, Y.C. Shan: Applied Mechanics and Materials, 268-270, 2012, 269-274. https://doi.org/10.4028/www.scientific.net/amm.268-270.269
75. E.L. Dalibon, D. Heim, Ch. Forsich, S.P. Brühl: Procedia Materials Science, 9, 2015, 163-170. https://doi.org/10.1016/j.mspro.2015.04.021
76. F.C. Nascimento, C.E. Foerster, S.L.R da Silva, C.M. Lepienski, C.J.M. Siqueira, C.A. Junio: Materials Research, 12(8), 2009, 173-180. https://doi.org/10.1590/s1516-14392009000200011